Word count: 8404 Revision: 2

Experiments on two techniques for the removal of barite from detrital zircon

Aaron J. Martin, Edna L. Guerrero-Juarez, Claudia L. Rocha-Estopier

División de Geociencias Aplicadas, IPICYT, CP 78216, San Luis Potosí, S.L.P., MEXICO

Martin is corresponding author. E-mail: aaron.martin@ipicyt.edu.mx

KEYWORDS

tenacity; sandstone; mineral separation; bias; provenance; maximum depositional age

ABSTRACT

Barite ($BaSO_4$) is a common mineral in sandstone that must be removed during separation of detrital zircon ($ZrSiO_4$). One widespread technique for the removal of barite exploits its lesser tenacity by milling the barite and zircon mixture in a ball mill. Here we test the extent to which such milling affects zircon and thus whether the milling could introduce bias into the detrital zircon sample. We then describe a new chemical technique for the removal of barite from detrital zircon. We find that milling a mixture of barite and zircon both breaks and causes loss of zircon grains, potentially introducing bias into a detrital zircon sample. Boiling barite in a 0.94 molar aqueous solution of sodium carbonate for four hours converts most grains to barium carbonate. The barium carbonate grains are opaque white and thus visually distinguishable from zircon, allowing separation by hand under a stereoscopic microscope. Alternatively, the barium carbonate grains can be dissolved by boiling in sixteen weight percent nitric acid for thirty minutes. In our experiments, boiling zircon in sodium carbonate solution and/or concentrated (sixty-five weight percent) nitric acid cleaned the surfaces of and the cracks in the grains but did not visibly change the zircon surfaces in other ways. Boiling only in concentrated nitric acid did not measurably affect the U-Pb and Lu-Hf isotopic systems in zircon interiors and boiling in a sodium carbonate solution followed by nitric acid did not detectably alter the Lu-Hf isotopic system. However, boiling in a concentrated sodium carbonate solution followed by nitric acid did disturb the U-Pb isotopic system in zircon interiors. Our results highlight the importance of proper technique during zircon isolation to minimize the introduction of bias into the sample.

INTRODUCTION

Barite ($BaSO_4$) is a common mineral in sandstone; it must be removed during isolation of detrital minerals such as zircon ($ZrSiO_4$). Separation of barite from zircon is challenging because of similar densities (mostly 4.4-3.9 g/cm^3 for barite and 4.7-4.2 g/cm^3 for zircon; Murakami et al., 1991; Schmidt et al. 2009; Shahab et al., 2016) and magnetic susceptibilities (Rosenblum and Brownfield, 1999). Barite is diamagnetic and zircon is diamagnetic to weakly paramagnetic (Krishnan et al., 1933; Lewis and Senftle, 1966; Sircombe and Stern, 2002). Barite additionally has low solubility in common solvents such as nitric, hydrochloric, and hydrofluoric acids at typical laboratory conditions, so it cannot be eliminated easily by direct dissolution (O'Neil, 2013). Although barite is soluble in hot concentrated sulfuric acid (Gaubert, 1909; Trenner and Taylor, 1930; O'Neil, 2013), most geologists choose not to use this solvent for routine mineral separation because it is difficult to handle safely. Barite is also soluble in organic acids such as diethylene triamine pentaacetic acid (DTPA; Putnis et al., 2008), but geologists likewise rarely use these solvents for mineral separation, perhaps because the effect of exposure to these organic acids on isotopic systems in zircon is unknown. Consequently, a mixture of barite and zircon often remains after all other minerals from the sandstone have been purged via techniques based on differences in density, magnetic susceptibility, and solubility in inorganic acid such as nitric acid. As the final step in the separation procedure, the standard technique in some laboratories for removing barite from detrital zircon exploits the markedly lesser tenacity of barite by milling the zircon and barite mixture in a ball mill, preferentially breaking the barite crystals (e.g., Gehrels et al., 2011). The milling continues until the barite grains are small enough to separate from the zircon by sieving.

Milling the zircon and barite mixture is a widespread practice and some geologists may assume that the zircon is not significantly broken because of its greater tenacity. However, the extent of comminution and loss of zircon grains during milling in a ball mill followed by sieving has not been tested. If zircon is broken and lost during the milling and subsequent sieving, this process can introduce bias into the detrital zircon population due to both the loss of grains and the possibility of dating several fragments of the same crystal but mistakenly classifying those fragments as separate detrital grains.

In this article we present the results of experiments that test for breakage and loss of zircon during milling with barite in ball mills. We then introduce a new method to chemically remove barite. Finally, we describe the results of experiments to examine the effects of the chemical method on zircon.

MILLING ZIRCON AND BARITE IN A BALL MILL

Design of experiments

To test the effect of milling on zircon, we used doubly-terminated zircon crystals so that any breakage of grains during milling would be apparent by visual examination of the crystals after milling. These grains came from a mafic dike that intruded Paleozoic sedimentary rocks in western Morocco (sample 58T in Domenech et al., 2016). The doubly-terminated crystals had no obvious microscopic fractures on their surfaces prior to milling (Fig. 1). For the experiments, we combined the zircon with natural barite, which we bought from a commercial supplier. The purchased barite grain was approximately 3 cm in diameter, so we crushed it to sand-size grains by hand using a ceramic mortar and pestle. We performed two sets of experiments using these zircon and barite crystals, one set in the UTChron Geo- and Thermochronometry Laboratory at

the University of Texas-Austin and the other in the Arizona LaserChron Center at the University of Arizona (Table 1). Our procedures followed the standard operating practices in each laboratory.

In the UTChron Laboratory, we first placed 100 doubly-terminated zircon crystals in each of two 2.54 cm-long polystyrene vials designed for use in a Wig-L-Bug® mill. For experiment UT1X, we added approximately the same volume of barite to the vial. For experiment UT10X, we added barite equal to approximately ten times the volume of the zircon. The range of barite grain sizes was similar to the range of zircon grain sizes, and barite volumes were estimated visually. We then added three acrylic plastic 3.2 mm-diameter spheres to each capsule and closed the vial with its cap. The milling thus took place in air in both experiments. We placed the sealed vial in the arms of an analog Wig-L-Bug® amalgamator model 3110-3A, made by Crescent Dental Manufacturing Company.

Experiment UT1X consisted of 10 minutes of shaking at 55% power. We then removed the vial from the machine and emptied the contents onto nylon mesh with openings of 30 μm. We used ethanol to remove all particles from the inside of the vial. Next, we used the ethanol to drive the fine particles through the mesh, leaving the coarser grains atop the mesh. Finally, we allowed the ethanol on the coarse grains to evaporate completely and poured the coarse grains onto wax paper for transport to the imaging facility.

Experiment UT10X involved two milling stages. First, we milled the barite and zircon mixture for 30 minutes at 55% power, followed by sieving using ethanol as described for experiment UT1X. Barite was still present in the coarse fraction atop the mesh, so after drying the grains we put them in another polystyrene vial with three acrylic plastic spheres for further milling. The second stage consisted of an additional 10 minutes of agitation at 55% power,

followed by sieving and drying as for experiment UT1X. After this step, barite was not visible in the coarse fraction, so we poured the coarse grains onto wax paper for transport to the imaging facility.

In the Arizona LaserChron Center, we first placed doubly-terminated zircon crystals into two pieces of wax paper, 100 grains into each paper. For experiment UA1X, we added approximately the same volume of barite as zircon to one of the pieces of wax paper. For experiment UA10X, we added approximately ten times the volume of barite as zircon to the other piece of wax paper. The range of barite grain sizes was similar to the range of zircon grain sizes, and barite volumes were estimated visually. Milling took place in a custom-built titanium capsule with an external diameter of 1.2 cm and an external length of 3.1 cm. We milled each sample with ten 3.2 mm-diameter acrylic plastic spheres in an analog Dentsply Caulk Vari-Mix III® amalgamator at low speed. Each sample was milled for three minutes in air followed by an additional three minutes in isopropyl alcohol. The contents of the capsule were then dumped onto sieve mesh with openings of 20 μm and the interior of the capsule rinsed with acetone to ensure all grains exited the capsule. Acetone was used to drive small mineral fragments through the sieve mesh. The acetone on the coarse grains atop the sieve mesh was allowed to evaporate and then the dry coarse grains were poured onto a piece of wax paper for transport to the imaging facility.

After milling, we examined and counted the grains using the optical microscope facilities at the Instituto Potosino de Investigacion Cientifica y Tecnologica (IPICYT). We also imaged the grains using the FEI Quanta 200 scanning electron microscope at IPICYT.

Results

Milling the barite and zircon mixture caused loss of zircon grains in all our experiments. Milling for 10 minutes in air resulted in loss of 24% of the zircon grains, whereas milling for 40 minutes in air caused loss of 49% of the zircon crystals (Table 1). Similarly, milling for three minutes in air followed by three minutes in isopropyl alcohol resulted in the loss of 36% of the zircon crystals in experiment UA1X and 30% in experiment UA10X (Table 1). One possible mechanism for zircon loss is the same as that for barite: comminution to a size small enough to pass through the mesh, then loss during sieving.

Examination of the zircon that remained after milling and sieving confirmed that the milling fractured some of the crystals. Some of the remaining zircon grains were unbroken (Fig. 2). However, in all the experiments, milling the barite and zircon mixture removed some of the zircon crystal tips and ruptured through the interiors of other grains (Figs. 2, 3). Of the zircon that remained after milling, 41% and 57% of the crystals were broken after milling for 10 and 40 minutes, respectively, in air (Table 1). Similarly, 64% and 23% of the remaining grains in experiments UA1X and UA10X, respectively, were broken after milling for three minutes in air followed by three minutes in isopropyl alcohol (Table 1). The surfaces of most milled grains host microscopic fractures that are not present on the surfaces of un-milled crystals (compare figures 1 and 3).

DISSOLUTION OF BARITE USING SODIUM CARBONATE SOLUTION FOLLOWED BY NITRIC ACID

Design of experiments

We used the natural barite described in the previous section for these experiments. Breit et al. (1985) described a two-step method for dissolving barite; we used their method as a guide

for developing our technique. The first step comprises conversion of the barite (barium sulfate) to barium carbonate by boiling in an aqueous solution of sodium carbonate according to the following reaction.

$$BaSO_4\ (s) + Na_2CO_3\ (aq) \leftrightarrow BaCO_3\ (s) + Na_2SO_4\ (aq) \quad (1)$$

The second step entails dissolution of the barium carbonate by hot nitric acid as shown in the following reaction.

$$BaCO_3\ (s) + 2HNO_3\ (aq) \leftrightarrow Ba(NO_3)_2\ (aq) + CO_2\ (g) + H_2O\ (l) \quad (2)$$

We tested the progress of reaction 1 at sodium carbonate solution concentrations of 1.9 M and 0.94 M for times ranging from eight hours to ten minutes. Experiments testing reaction 1 used the following procedure.

1. Add 2 or 1 g fine-grained sodium carbonate to 10 mL deionized water in a 30 mL Pyrex beaker. It is necessary to gently warm the water after addition of the sodium carbonate to allow 2 g of sodium carbonate to dissolve in 10 mL of water. Stir until all the sodium carbonate is dissolved. Dissolving 2 g of sodium carbonate in 10 mL of water yields a concentration of 1.9 M and 1 g of sodium carbonate produces a concentration of 0.94 M.
2. Add 100 mg of sand-sized barite grains.
3. Cover with a watch glass and boil. If evaporation causes the solution level to approach the bottom of the beaker, add more deionized water as necessary.

4. While still warm, decant the supernatant liquid. Rinse the grains ten times with 30 mL of deionized water each time. The rinsing removes the sodium sulfate and remaining sodium carbonate.
5. Allow the grains to dry.

After the completion of step 5, we divided the grains into two aliquots. We saved the first aliquot for further testing. We cast the second aliquot in an epoxy disk and then polished into the interiors of the grains. Finally, we examined the interiors of the grains using the scanning electron microscope at IPICYT.

We boiled in nitric acid only the grains that had been boiled in the sodium carbonate solution for four and eight hours. We used the following procedure to implement reaction 2.

1. Add 30 mL of concentrated (65 wt%) nitric acid to a 30 mL Pyrex beaker.
2. Add the grains that resulted from reaction 1.
3. Cover with a watch glass and boil for one hour. It was not necessary to add more acid during boiling because evaporation did not cause the acid level to approach the bottom of the beaker.
4. Decant the acid and rinse ten times with 30 mL deionized water each time.

Results

For reaction 1, boiling times less than four hours resulted in only partial conversion of the barite to barium carbonate, whereas boiling for four or eight hours completely converted most crystals to barium carbonate (Figs. 4, 5). Both sodium carbonate concentrations resulted in conversion of most crystals to barium carbonate after boiling for four or eight hours (Fig. 5).

Examination of the partially-converted grains after boiling for two and three hours revealed a barite core surrounded by a barium carbonate crust (Fig. 4). Some grains additionally contained a mantle of partially-altered barite between the core and the crust (Figs. 4B, 4C). In a few grains we examined, there also was a linear region composed of barium carbonate that crossed the interior of the barite grain (Figs. 4B, 4C). The barium carbonate crust was opaque white and thus visually distinguishable from both barite and zircon when viewed in reflected light. This crust was present on all grains after boiling in the sodium carbonate solution for at least two hours.

After boiling the products of reaction 1 (four and eight hours) for one hour in concentrated nitric acid, most grains disappeared. The few remaining grains were smaller than the largest grains prior to implementing reactions 1 and 2. Examination of the remaining grains in the scanning electron microscope revealed that they are barite crystals with scalloped and pitted surfaces (Fig. 6).

EFFECTS OF SODIUM CARBONATE SOLUTION AND NITRIC ACID ON ZIRCON

Design of experiments

In order to be useful for the isolation of detrital zircon from real samples, the new chemical method for eliminating barite cannot affect the chemical elements of interest in the zircon. We carried out two sets of experiments to test the impacts on zircon of boiling in sodium carbonate solution and/or concentrated nitric acid. We performed these experiments on zircon alone in order to focus on the possible effects of these chemicals on zircon without complications from reactions with other minerals. Although the degree of crystallinity likely controls key aspects of reactions between zircon and these chemicals (cf. Mattinson, 2005), we did not

measure the degree of crystallinity in the studied zircon. However, the standard reference zircon crystals used for the second set of experiments have different degrees of crystallinity due to their different ages and radiogenic element contents, so in these experiments we tested the response of zircon with different degrees of metamictization to boiling in sodium carbonate solution and/or concentrated nitric acid.

Visible changes to the surface of zircon – methods. In the first set of experiments, we searched for changes to zircon surfaces visible in backscattered and secondary electron images. We purchased cm-long zircon crystals from a commercial supplier and imaged the surfaces of three grains prior to boiling in sodium carbonate solution and/or concentrated nitric acid. We then examined the surfaces of the zircon crystals after the following experiments, which we conducted following the steps listed in the previous section. (A) We boiled one zircon crystal for eight hours in a 1.9 M aqueous solution of sodium carbonate only. (B) We boiled a second zircon crystal for one hour in concentrated nitric acid only. (C) We boiled the third zircon crystal in a 1.9 M sodium carbonate solution for eight hours followed by boiling in concentrated nitric acid for one hour. After rinsing and drying, we prepared each of the three grains for the second round of imaging in the scanning electron microscope.

Changes to isotopic systems in zircon interiors – methods. In the second set of experiments, we analyzed the effects on the U-Pb and Lu-Hf isotopic systems in zircon of boiling in a sodium carbonate solution and/or concentrated nitric acid. We chose these systems because they are some of the most commonly analyzed isotopic systems in zircon. We used standard reference zircon FC-1, Sri Lanka, R33, and Plesovice to test for effects on the U-Pb

system. For the Lu-Hf system, we used these four standards plus Mud Tank. We chose these standards because of their wide ranges of uranium concentrations, crystallization ages, Lu/Hf ratios, and $^{176}Hf/^{177}Hf$ ratios (Table S1). Our two experiments entailed (A) one hour of boiling in concentrated nitric acid only, and (B) boiling for four hours in a 1.9 M sodium carbonate solution followed by boiling for one hour in concentrated nitric acid. For experiment B, after boiling in the sodium carbonate solution, we allowed the zircon to remain in the solution at room temperature for seven days to increase the extent of any reaction that might have occurred between the zircon and the sodium carbonate. After boiling, we rinsed the zircon with deionized water and then allowed the grains to dry.

After the experiments, we placed the zircon on double-sided tape by hand while viewing the crystals under a stereo microscope. We divided the zircon grains onto three different pieces of tape based on grain size: large, medium, and small. This division is indicated in the name of each analysis in Tables S2 and S3 using the words “Big”, “Med”, and “Small”. We then placed shards of zircon standards FC-1 and R33 on the tape for use during U-Pb data acquisition. We cast these grains into an epoxy disk and then polished into the interiors of the grains by hand using sandpaper.

We acquired U-Pb and Lu-Hf isotope data using the same laser ablation system and mass spectrometer in the Arizona LaserChron Center at the University of Arizona. Details of the mass spectrometry techniques were given in Gehrels and Pecha (2014), Pullen et al. (2014), and Ibanez-Mejia et al. (2015), so we only briefly summarize them here. We first acquired U-Pb isotope data from spots in twelve different zircon crystals from each of the experiments over the course of a single day. The following day, we obtained Lu-Hf isotope data from spots at least 40 μm away from the U-Pb ablation pits (measured from the edges of each pit) in ten to eleven

different zircon grains from each of the experiments. The only exceptions were for Lu-Hf isotopes in experiment Sod-R33, in which spots med5 and med9 were placed in the same grain, and spots med6 and med10 likewise were located in another single grain (Table S3).

We used a Photon Machines Analyte G2 excimer laser attached to a HelEx cell to ablate the zircon. The laser beam diameter was 30 μm for U-Pb isotopes and 40 μm for Lu-Hf isotopes. The laser fired seven bursts per second, which produces a zircon ablation rate of 0.4 μm/s (Ibanez-Mejia et al., 2015). U-Pb analysis required 108 total bursts whereas Lu-Hf analysis used 455 total bursts. For U-Pb isotope data acquisition, one analysis of standard reference zircon FC-1 bracketed every four analyses of zircon from the experiments. The analyses of FC-1 were used to correct for fractionation of U and Pb isotopes. Standard reference zircon R33 was analyzed twice at the beginning and again at the end of the group of analyses from each of our three mounts. The R33 analyses were used to check the quality of the data acquisition procedures. For Lu-Hf isotope analysis, we bracketed twenty spots in experiment zircon with one spot in each of the following seven zircon standards: FC-1, Plesovice, 91500, Temora, R33, Sri Lanka, and Mud Tank.

The ablated zircon was carried into the plasma source of a Nu Instruments high resolution multi-collector inductively coupled plasma mass spectrometer in helium gas. For the U-Pb analyses, ^{204}(Pb+Hg) and ^{202}Hg were determined using ion counters and ^{238}U, ^{232}Th, ^{208}Pb, ^{207}Pb, and ^{206}Pb were measured in Faraday cups. For the Lu-Hf analyses, all necessary isotopes were measured using Faraday cups.

Data reduction was performed offline using numerical routines written in-house at the Arizona LaserChron Center (Sundell et al., 2020). Correction for common lead was performed using values interpreted from Stacey and Kramers (1975). Correction for interference with ^{176}Hf

282 by ^{176}Lu and ^{176}Yb was performed as recommended by Woodhead et al. (2004). All
283 uncertainties are discussed at the 95% confidence level unless otherwise noted.
284 We calculated weighted means and associated mean squared weighted deviation
285 (MSWD) values using Isoplot 4.15 (Ludwig, 2008). A t-test measured the probability that the
286 means of the analyses of the boiled zircon differed from the means of analyses of untreated
287 zircon. Table 2 lists the sources of the analyses of untreated zircon; for the data from Sundell et
288 al. (2020), we used only the data acquired at the rate of 30 seconds per analysis because this
289 matches our acquisition rate. We calculated the associated p-value using the t.test function in
290 Excel, selecting the parameters for two-tailed, heteroscedastic tests.
291
292 **Results**
293 **Visible changes to the surface of zircon – results.** Figure 7 shows backscattered and
294 secondary electron images of the surface of a large zircon crystal before and after boiling in a 1.9
295 M sodium carbonate solution for eight hours. The zircon itself shows no obvious change.
296 However, the removal of the dark gray to black spots visible in figure 7A indicates that the
297 treatment did remove surface contamination. The process also made the cracks more prominent
298 (Figs. 7C and 7D). The increased prominence is due to removal of material from the cracks, not
299 widening.
300 Figure 8 shows backscattered and secondary electron images of the surface of a large
301 zircon crystal before and after boiling in concentrated nitric acid for one hour. The zircon itself
302 shows no obvious change. Like the treatment with sodium carbonate solution, boiling in
303 concentrated nitric acid did remove contaminants from the surface of the zircon (Figs. 8A and
304 8B) as well as from cracks (Figs. 8C and 8D). The increased prominence of the cracks on the

surface of the crystal (cf. Figs. 8C and 8D) is due to this removal of material, not widening of the cracks.

Figure 9 shows backscattered and secondary electron images of the surface of a large zircon crystal before and after boiling in sodium carbonate solution followed by boiling in concentrated nitric acid. As for the other treatments, this process removed contaminants from the surface of and cracks in the zircon, but apparently did not affect the zircon crystal itself. Figures 9E and 9F demonstrate the removal of material from cracks in detail. After the boiling steps, the cracks were deeper and the boundaries between the crystal and the cracks were sharper, but the cracks were not wider.

Changes to isotopic systems in zircon interiors – results. We dated untreated FC-1 and R33 grains as part of the normal U-Pb isotope data acquisition procedure used for all samples analyzed on the Nu Instruments mass spectrometer in the Arizona LaserChron Center. The combined results from analyses of these standards on all three of our mounts are shown in Figure S1 and Table 2. The analyses of untreated FC-1 produced a weighted mean date older than the published age outside uncertainties. The MSWD of these analyses was 2.3. Of the twelve analyses of untreated R33, we recognize one as poor because its $^{206}Pb/^{238}U$ date is far from the published age and very different than the other dates from untreated R33. This analysis is marked in red, struck-through text in Table S2 and we did not include it in the summaries in Figure S1 and Table 2, nor for the calculations of p-values when comparing the analyses of boiled and unboiled standards. The remaining eleven analyses yielded a weighted mean date that only barely overlapped the published age within uncertainties, with an MSWD of 3.4.

This is the peer-reviewed, final accepted version for American Mineralogist, published by the Mineralogical Society of America.
The published version is subject to change. Cite as Authors (Year) Title. American Mineralogist, in press.
DOI: https://doi.org/10.2138/am-2021-7436. http://www.minsocam.org/

Isotopic analyses of the interiors of the boiled standard zircon grains produced weighted mean $^{206}Pb/^{238}U$ dates within uncertainty of the published ages in most cases (Figs. S1, S2; Tables 2, S1). There were three exceptions: FC-1 boiled in sodium carbonate solution then concentrated nitric acid, and R33 from both types of experiments. There was small to moderate scatter in the dates from the individual analyses of each boiled standard, with MSWD values between about 4 and 1 (Figs. S1, S2; Table 2). R33 analyses yielded a moderately high degree of dispersion in both experiments whereas analysis of Plesovice consistently resulted in low variance. The p-values for analyses of FC-1, R33, and Plesovice boiled in concentrated nitric acid alone were high to moderate, 0.94 to 0.06 (Table 2). In contrast, the p-values for analyses of FC-1, R33, and Plesovice boiled in sodium carbonate solution followed by nitric acid were low, 0.03 to 0.0004. The p-values for analyses of Sri Lanka were low in both cases. There were only two obviously poor U-Pb analyses; these are marked in red, struck-through text in Table S2. Both came from R33, one analysis from each of the two types of experiments. We identify these analyses as poor because their dates are both far from the published age and very different than the other dates from the boiled R33 crystals. These analyses are not shown in Figure S1 and were not included in the calculations of the weighted mean dates and the MSWD and p-values.

Isotopic analyses of untreated standard reference zircon yielded weighted mean $^{176}Hf/^{177}Hf$ ratios that overlapped the published values for six of the seven standards; the exception was Temora (Fig. S3; Tables 2, S1). MSWD values for the analyses of untreated zircon ranged from 6.1 to 0.4.

The weighted mean $^{176}Hf/^{177}Hf$ ratios of the zircon subjected to boiling in sodium carbonate solution and/or concentrated nitric acid likewise mostly overlapped the published values (Fig. S3; Tables 2, S1). MSWD values ranged from 6.8 to 1.5. P-values of analyses from

all but one of the boiled standards were high, between 0.95 and 0.19. The exception was FC-1 boiled in sodium carbonate solution followed by concentrated nitric acid; the p-value for these analyses was 0.042.

APPLICATION TO A NATURAL SAMPLE

Design of experiment

In order to verify that the chemical technique described in this paper effectively removes barite from detrital mineral separates derived from natural sandstone samples, we applied reactions 1 and 2 to grains separated from a sample of barite-rich sandstone. The sandstone sample was collected from the upper part of the Alamar Formation exposed approximately 15 km south of Galeana, Nuevo Leon, Mexico (Barboza-Gudino et al., 2014). The sample location was 24.6969 °N, 100.1013 °W. The outcrop contains barite veins (Kesler et al., 1988; Kroeger and Stinnesbeck, 2003).

The separate shown in Figure 10A was produced as follows. First, an approximately 1 kg sample was crushed by hand using a stainless steel mortar and pestle. Clay- and silt-sized particles were then removed by hand panning in water. Next, the sand-sized grains were passed through a Frantz magnetic barrier separator in steps at 0.5, 1.0, and 1.8 A. Finally, the non-magnetic grains were placed in room temperature LST Heavy Liquid (aqueous solution of lithium heteropolytungstates) for density separation. The dense grains were used for further processing and are shown in Figure 10A. During isolation of detrital zircon, quartz grains sometimes remain after the magnetic and dense liquid separation steps. We left a moderate amount of quartz in the separate to test whether quartz affects the progress of reaction 1 and/or reaction 2 (Fig. 10).

To apply reactions 1 and 2 to the separate shown in Figure 10A, we followed the steps listed in a previous section. We first boiled the grains in a 0.98 M sodium carbonate solution for four hours. We then boiled the grains in concentrated nitric acid for one hour. We imaged the grains in reflected light before and after these processes (Fig. 10)

Results

Figure 10 shows the results of our experiment on separates from a natural barite-bearing sandstone sample. Prior to the treatment, the separate contained so much barite that it was difficult to distinguish zircon (Fig. 10A). The treatment nearly completely removed the barite, making zircon grains much easier to identify (Fig. 10B). Quartz grains appear not to have been affected by the reactions.

DISCUSSION

Problems with physical removal of barite by milling then sieving

In all four ball mill experiments, milling a mixture of barite and zircon fractured the zircon along with the barite (Figs. 2, 3). Loss of zircon also occurred during all four ball mill experiments (Table 1). We infer that sieving separated the newly-formed small fragments of zircon, which were produced during milling, from the larger grains, causing loss of the small pieces of zircon from the sample. As expected if this explanation for zircon loss is correct, more grains were lost after 40 minutes than after 10 minutes of milling (experiments UT10X versus UT1X). Further, more of the remaining grains were broken after 40 minutes of milling. Microscopic cracks on the surfaces of the remaining zircon grains likely resulted from the milling (Fig. 3). If so, these microscopic fractures attest to the damage that milling causes to

zircon. Because of the ubiquity of lost and fractured grains in our four experiments, we suggest that zircon loss and breakage may be common in zircon subjected to ball milling in general, even for moderate durations such as six or ten minutes.

Losing zircon grains can introduce bias into the sample because the lost grains are not available for dating. Breaking the grains also can introduce bias even if the broken fragments are retained because if a geologist dates each fragment, the dates incorrectly will be treated as coming from separate grains, although in fact they were a single detrital grain in the sandstone. That is, a geologist would obtain two or more dates from a single detrital grain without realizing that the dates all came from the same detrital grain. Even losing the tips of zircon grains is unacceptable if the project goals require analyzing the tips.

Fewer of the remaining zircon crystals were broken during experiment UA10X than during experiment UA1X (Table 1). We infer that the greater volume of barite in experiment UA10X reduced the number and/or speed of collisions between zircon and the plastic balls compared to experiment UA1X, leaving fewer fractured zircon grains at the end of the six-minute milling period.

Controls on the transformation of barite to barium carbonate

The conversion of barite to barium carbonate by reaction 1 apparently proceeded from the grain edges into the grain interiors, as indicated by several observations. First, after boiling in a sodium carbonate solution for at least 2 hours, all former barite grains were either completely converted to barium carbonate or coated with a barium carbonate crust. Second, figures 4B and 4C show one grain with a barite core surrounded by a mantle of partially-altered barite overlain by a crust of barium carbonate. The complete conversion of the rims of all the

grains after boiling for at least 2 hours as well as the decreasing conversion extent with depth into the large grains suggests that the reaction proceeded inward from the grain edges.

Boiling for more than four hours in the sodium carbonate solution did not noticeably increase the fraction of grains completely converted to barium carbonate. Similarly, boiling in a 1.9 M rather than a 0.94 M sodium carbonate solution did not noticeably increase the fraction of completely converted grains. These results indicate that permeability is the limiting factor for complete conversion of grains given sufficient time and sodium carbonate concentration. In this scenario, after boiling for four hours in a 0.94 M solution, all sectors of the barite crystals that can be accessed by the sodium carbonate solution have been converted to barium carbonate. The parts of the crystals that have not been converted to barium carbonate are not reachable by the sodium carbonate solution, and boiling for more time or at a greater sodium carbonate concentration does not make those inaccessible parts of the crystals more accessible. That is, boiling for more time or at a greater sodium carbonate concentration does not increase the permeability of each grain. The linear feature composed of barium carbonate that enters the interior of the crystal in figures 4B and 4C appears to be a former fracture. This and similar features in other grains suggest that fractures may facilitate reaction 1 in barite crystal interiors, presumably by increasing permeability.

The grains that remained after treatment with reactions 1 and 2 were heavily scalloped and pitted barite crystals (Fig. 6). We infer that these grains were barite crystals too large and too impermeable for complete conversion to barium carbonate because the sodium carbonate solution could not penetrate into all parts of the interiors of the grains.

Effects of boiling zircon in sodium carbonate solution and nitric acid

442 **Visible changes to zircon grain surfaces.** Boiling in sodium carbonate solution and/or
443 in concentrated nitric acid did not noticeably change the appearance of zircon surfaces (Figs. 7,
444 8, 9). However, boiling in each chemical cleaned zircon surfaces of contaminants. Boiling in
445 concentrated nitric acid appeared to remove more material from cracks as compared to boiling in
446 sodium carbonate solution.
447
448 **U-Pb isotope analyses.** The weighted mean $^{206}Pb/^{238}U$ dates from the boiled standard
449 zircon crystals were not identical to the published ages, and the MSWD values for the analyses
450 from half the boiled standards were between 4 and 2 (Figs. S1, S2; Tables 2, S1). For our
451 purposes, the relevant question is how much of these measured age offsets and dispersions were
452 caused by the treatment with sodium carbonate solution and/or nitric acid and how much were
453 the results of other factors such as natural variability in the standard zircon and artifacts
454 introduced during isotope analysis. The main tool we use to answer this question is to compare
455 the results of the U-Pb isotope measurements of the boiled zircon standards to U-Pb isotope data
456 from the same zircon standards not subjected to any experiments and acquired on the same mass
457 spectrometer. The t-test p-values summarize this comparison.
458 The p-values for the analyses of FC-1, R33, and Plesovice subjected to boiling in nitric
459 acid alone were high to moderate, suggesting that boiling only in concentrated nitric acid did not
460 change the mean $^{206}Pb/^{238}U$ date of each standard. In contrast, the p-values for the analyses of
461 these standards boiled in sodium carbonate solution followed by nitric acid were low; the p-value
462 for analyses of each standard boiled in both chemicals was at least an order of magnitude lower
463 than the p-value for analyses of the same standard boiled only in nitric acid. This reduction in p-
464 values for analyses of all three standards to values less than 0.03 suggests that boiling in sodium

carbonate solution followed by nitric acid affected the U-Pb isotopic system in these zircon standards. For all three standards, the direction of change was toward younger $^{206}Pb/^{238}U$ dates for the standards subjected to boiling in both chemicals compared to the same standards boiled only in nitric acid and compared to the published age.

P-values were low for analyses of Sri Lanka grains in both experiments. We attribute these low p-values to heterogeneity in the $^{206}Pb/^{238}U$ dates in the Sri Lanka zircon, as indicated by the different published crystallization ages of this standard (Table S1). Our weighted mean dates and uncertainties of 556±2 Ma (concentrated nitric acid only) and 555±3 Ma (sodium carbonate solution then concentrated nitric acid) overlap the 560-557 Ma crystallization age published by Santos et al. (2017) but not the 564±3 Ma crystallization age published by Gehrels et al. (2008). For determining p-values, all the published analyses to which we compared ours were closer to the 564 Ma age, and our low p-values confirm that the means from our analyses are not equivalent to the 564 Ma age. We speculate that we may have used shards of Sri Lanka zircon with ages more similar to those found by Santos et al. (2017) than by Gehrels et al. (2008) in our experiments.

In summary, boiling in concentrated nitric acid alone did not measurably affect the U-Pb isotopic system in the studied zircon. In contrast, boiling in an aqueous solution of sodium carbonate followed by concentrated nitric acid appears to have disturbed the U-Pb isotopic system in the studied zircon standards, resulting in a small decrease in the measured mean $^{206}Pb/^{238}U$ date. Our experiments on standard zircon in sodium carbonate solution used a more aggressive procedure than necessary for removing barite – we used double the required sodium carbonate concentration and then we allowed the zircon to remain in the sodium carbonate solution at room temperature for a week after boiling. It is possible that the less aggressive

technique required for barite removal would not measurably affect the U-Pb isotopic system in zircon.

Lu-Hf isotope analyses. The high p-values from nine of our ten experiments demonstrate that boiling in sodium carbonate solution and/or concentrated nitric acid did not significantly shift the mean $^{176}Hf/^{177}Hf$ ratios relative to the mean $^{176}Hf/^{177}Hf$ ratios we measured in the untreated standard zircon. Further, the weighted mean $^{176}Hf/^{177}Hf$ ratios of the boiled zircon overlapped the published values within uncertainties. Although there was much more scatter in measurements of the $^{176}Hf/^{177}Hf$ ratio in five experiments on standard zircon than in untreated standard zircon, there was similar or less scatter in the other five experiments. We therefore conclude that boiling in sodium carbonate solution and/or concentrated nitric acid did not demonstrably affect the Lu-Hf isotopic system in the studied standard zircon.

Comments and recommended workflow

The removal of barite from detrital zircon without negatively affecting the zircon remains a thorny problem. One option, milling in a ball mill, breaks and removes zircon along with barite, potentially introducing bias into the zircon separate. The technique described in this paper, dissolution of barite by boiling in a sodium carbonate solution followed by concentrated nitric acid, disturbs the U-Pb isotopic system in zircon for a concentration of sodium carbonate higher than necessary for barite dissolution. If future research shows that boiling at the lower concentration needed for barite dissolution does not affect the U-Pb system in zircon, the method described in this paper would appear to be preferable to milling for barite removal. The

chemical method did not disturb the Lu-Hf isotopic system in zircon, so this technique appears viable for studies that make use of the Lu-Hf isotopic system alone.

We recommend the following procedure in the event that a geologist chooses to remove barite from zircon using an aqueous solution of sodium carbonate followed by nitric acid.

1. In a Pyrex beaker, add 2 g of fine-grained sodium carbonate to 20 mL of deionized water. Agitate until the sodium carbonate is completely dissolved. Using 20 mL of deionized water rather than 10 mL confers the advantage that the water does not boil dry as quickly. If it is necessary to warm the water to allow complete dissolution, we recommend adding the sodium carbonate to the water prior to warming.
2. Add the detrital grains to the solution. If both the quantity and size of the grains are small, we recommend adding an inert bubble nucleator to reduce the likelihood of explosive bubble formation. Pebble-size quartz grains are an inexpensive bubble nucleator.
3. Cover the beaker with a watch glass and boil for four hours. If the level of the solution nears the bottom of the beaker, add deionized water as necessary.
4. Decant the solution and rinse ten times with 30 mL deionized water each time. Allow the remaining water to evaporate completely.
5. Add 20 to 30 mL 16 wt% nitric acid.
6. Cover the beaker with a watch glass and boil for thirty minutes.
7. Decant the acid and rinse ten times with 30 mL deionized water each time. Allow the remaining water to evaporate completely.

This process will remove most barite grains and greatly reduce the size of the large crystals. As shown in figure 6, any remaining barite grains will be corroded and visibly different from zircon. Accordingly, further chemical removal will not be necessary for most samples

because any remaining barite grains can be picked out by hand or avoided when choosing spots for in situ analysis. However, if desired, the chemical removal process can be performed a second time.

An alternative to applying both reactions 1 and 2 to a barite-bearing separate is to stop after the conversion to barium carbonate using reaction 1. Barium carbonate is opaque white and thus optically different than zircon. After the transformation using reaction 1, the barium carbonate grains can be picked out of the separate by hand or not selected for in situ analysis if mounted with zircon.

Hydrochloric acid dissolves barium carbonate (Breit et al., 1995; O'Neil, 2013), although we did not test hydrochloric acid as part of our procedure. We prefer hot nitric acid because it easily dissolves pyrite whereas hydrochloric acid does not (Lord, 1982; Huerta-Diaz and Morse, 1990). Pyrite commonly remains after separation based on differences in density and magnetic susceptibility and must be removed during zircon isolation. Using our procedure with nitric acid removes both barite and pyrite. Nitric acid also removes other minerals such as apatite that can persist in separates after density- and magnetic susceptibility-based separation steps (Evans et al., 2005). An additional benefit of utilizing our procedure is cleaning contaminants from zircon surfaces and cracks.

IMPLICATIONS

Milling in a ball mill is a common technique to eliminate barite from a detrital zircon sample. Our experiments demonstrated that such milling can introduce bias into the sample by breaking the zircon, resulting in loss of some zircon crystals and repetition of others. Conversion of the barite to barium carbonate using an aqueous solution of sodium carbonate as described in

this paper would be preferable if future research shows that this method, with a concentration of sodium carbonate just sufficient to convert the barite, does not affect the U-Pb isotopic system in zircon. However, the current situation is that there is no barite removal method that demonstrably does not negatively affect zircon. The finding that boiling in concentrated nitric acid for one hour did not affect the U-Pb or Lu-Hf isotopic systems in zircon supports the continued use of nitric acid for removal of pyrite and other minerals from detrital zircon.

ACKNOWLEDGEMENTS

Mireia Domenech-Verdaguer graciously provided the doubly-terminated zircon crystals and produced the separate shown in Figure 10. We thank Daniel F. Stockli, Lisa D. Stockli, and Rudra Chatterjee for use of microscopes and the Wig-L-Bug® mill, and George Gehrels, Mark Pecha, Nicky Giesler, Gayland Simpson, and Emma Kroeger for assistance with the Vari-Mix III® amalgamator and mass spectrometry in the Arizona LaserChron Center. We thank Alfredo Aguillon-Robles and Miguel Cortina-Rangel for facilitating access to the Frantz magnetic barrier separator in the Instituto de Geologia at the Universidad Autonoma de San Luis Potosi. At IPICYT, Mercedes Zavala-Arriaga assisted with microscopy, Victoria Gonzalez-Rodriguez helped with fume hood access, and Ana Iris Pena-Maldonado supported use of the electron microscope. The scanning electron microscope facility is part of the Laboratorio Nacional de Investigaciones en Nanociencias y Nanotecnologia. IPICYT provided partial funding for this research. This paper is based on Edna Guerrero-Juarez's master's thesis at IPICYT. Pablo Davila-Harris, Mireia Domenech-Verdaguer, and Nadia Martinez-Villegas contributed valuable comments on that thesis. Helpful reviews by Joel E. Saylor, an anonymous reviewer, and Associate Editor Paul Tomascak greatly improved the manuscript.

REFERENCES

Barboza-Gudino, J.R., Ocampo-Diaz, Y.Z.E., Zavala-Monsivais, A., and Lopez-Doncel, R.A., 2014, Procedencia como herramienta para la subdivision estratigrafica del Mesozoic temprano en el noreste de Mexico: Revista Mexicana de Ciencias Geologicas, v. 31, p. 303–324.

Breit, G.N., Simmons, E.C., and Goldhaber, M.B., 1985, Dissolution of barite for the analysis of strontium isotopes and other chemical and isotopic variations using aqueous sodium carbonate: Chemical Geology, v. 52, p. 333–336, doi:10.1016/0168-9622(85)90043-0.

Cui, H. et al., 2016, Environmental context for the terminal Ediacaran biomineralization of animals: Geobiology, v. 14, p. 344–363, doi:10.1111/gbi.12178.

Domenech, M., Teixell, A., and Stockli, D.F., 2016, Magnitude of rift-related burial and orogenic contraction in the Marrakech High Atlas revealed by zircon (U-Th)/He thermochronology and thermal modeling: Tectonics, v. 35, p. 2609–2635, doi:10.1002/2016TC004283.

Evans, N.J., Byrne, J.P., Keegan, J.T., and Dotter, L.E., 2005, Determination of uranium and thorium in zircon, apatite, and fluorite: Application to laser (U-Th)/He thermochronology: Journal of Analytical Chemistry, v. 60, p. 1159–1165, doi:10.1007/s10809-005-0260-1.

Gaubert, P., 1909, Sur la reproduction artificielle de la barytine, de la celestine, de l'anglesite, de l'anhydrite, et de l'hydrocyanite, et sur les modifications de leurs formes dominantes: Bulletin de la Societe Francaise de Mineralogie, v. 32, p. 139–149.

600 Gehrels, G.E., Blakey, R., Karlstrom, K.E., Timmons, J.M., Dickinson, B., and Pecha, M., 2011,
601 Detrital zircon U-Pb geochronology of Paleozoic strata in the Grand Canyon, Arizona:
602 Lithosphere, v. 3, p. 183–200, doi:10.1130/L121.1.
603 Gehrels, G., and Pecha, M., 2014, Detrital zircon U-Pb geochronology and Hf isotope
604 geochemistry of Paleozoic and Triassic passive margin strata of western North America:
605 Geosphere, v. 10, p. 49–65, doi:10.1130/GES00889.1.
606 Gehrels, G.E., Valencia, V.A., and Ruiz, J., 2008, Enhanced precision, accuracy, efficiency, and
607 spatial resolution of U-Pb ages by laser ablation-multicollector-inductively coupled
608 plasma-mass spectrometry: Geochemistry, Geophysics, Geosystems, v. 9, Q03017,
609 doi:10.1029/2007GC001805.
610 Huerta-Diaz, M.A., and Morse, J.W., 1990, A quantitative method for determination of trace
611 metal concentrations in sedimentary pyrite: Marine Chemistry, v. 29, p. 119–144,
612 doi:10.1016/0304-4203(90)90009-2.
613 Ibanez-Mejia, M., Pullen, A., Arenstein, J., Gehrels, G.E., Valley, J., Ducea, M.N., Mora, A.R.,
614 Pecha, M., and Ruiz, J., 2015, Unraveling crustal growth and reworking processes in
615 complex zircons from orogenic lower-crust: The Proterozoic Putumayo Orogen of
616 Amazonia: Precambrian Research, v. 267, p. 285–310,
617 doi:10.1016/j.precamres.2015.06.014.
618 Kesler, S.E., Jones, L.M., and Ruiz, J., 1988, Strontium and sulfur isotope geochemistry of the
619 Galeana barite district, Nuevo Leon: Economic Geology, v. 83, p. 1907–1917,
620 doi:10.2113/gsecongeo.83.8.1907.

621 Krishnan, K.S., Guha, B.C., and Banerjee, S., 1933, Investigations on magne-crystallic action.
622 Part I: Diamagnetics: Philosophical Transactions of the Royal Society A: Mathematical,
623 Physical and Engineering Sciences, v. 231, p. 235–262, doi:10.1098/rsta.1933.0007.
624 Kroeger, K.F., and Stinnesbeck, W., 2003, The Minas Viejas Formation (Oxfordian) in the area
625 of Galeana, northeastern Mexico: Significance of syndepositional volcanism and related
626 barite genesis in the Sierra Madre Oriental, *in* Bartolini, C., Buffler, R.T., and Blickwede,
627 J.F. eds., The Circum-Gulf of Mexico and the Caribbean: Hydrocarbon habitats, basin
628 formation, and plate tectonics, American Association of Petroleum Geologists, Memoir,
629 v. 79, p. 515–528.
630 Lewis, R.R., and Senftle, F.E., 1966, The source of ferromagnetism in zircon: American
631 Mineralogist, v. 51, p. 1467–1475.
632 Lord III, C.J., 1982, A selective and precise method for pyrite determination in sedimentary
633 materials: Journal of Sedimentary Research, v. 52, p. 664–666, doi:10.1306/212F7FF4-
634 2B24-11D7-8648000102C1865D.
635 Ludwig, K.R., 2008, User's manual for Isoplot 3.70: Berkeley Geochronology Center Special
636 Publication 4, 76 p.
637 Martin, A.J., Kadel-Harder, I., Owens, B.E., Kitajima, K., Samson, S.D., and Verma, S.K., 2020,
638 Five hundred million years of punctuated addition of juvenile crust during extension in
639 the Goochland Terrane, central Appalachian Piedmont Province: International Geology
640 Review, v. 62, p. 523–548, doi:10.1080/00206814.2019.1622156.
641 Martin, A.J., Southworth, S., Collins, J.C., Fisher, S.W., and Kingman, E.R.I., 2015, Laurentian
642 and Amazonian sediment sources to Neoproterozoic–lower Paleozoic Maryland
643 Piedmont rocks: Geosphere, v. 11, p. 1042–1061, doi:10.1130/GES01140.1.

644 Mattinson, J.M., 2005, Zircon U–Pb chemical abrasion ("CA-TIMS") method: Combined
645 annealing and multi-step partial dissolution analysis for improved precision and accuracy
646 of zircon ages: Chemical Geology, v. 220, p. 47–66, doi:10.1016/j.chemgeo.2005.03.011.
647 Murakami, T., Chakoumakos, B.C., Ewing, R.C., Lumpkin, G.R., and Weber, W.J., 1991,
648 Alpha-decay event damage in zircon: American Mineralogist, v. 76, p. 1510–1532.
649 O'Neil, M.J. (Ed.), 2013, The Merck index: an encyclopedia of chemicals, drugs, and
650 biologicals, 15th ed: Cambridge, UK, Royal Society of Chemistry, 2708 p.
651 Pullen, A., Ibanez-Mejia, M., Gehrels, G.E., Ibanez-Mejia, J.C., and Pecha, M., 2014, What
652 happens when n=1000? Creating large-n geochronological datasets with LA-ICP-MS for
653 geologic investigations: Journal of Analytical Atomic Spectrometry, v. 29, p. 971–980,
654 doi:10.1039/c4ja00024b.
655 Putnis, C.V., Kowacz, M., and Putnis, A., 2008, The mechanism and kinetics of DTPA-promoted
656 dissolution of barite: Applied Geochemistry, v. 23, p. 2778–2788,
657 doi:10.1016/j.apgeochem.2008.07.006.
658 Rosenblum, S., and Brownfield, I.K., 1999, Magnetic susceptibilities of minerals: U.S.
659 Geological Survey Open-File Report 99–529, 37 p.
660 Santos, M.M. et al., 2017, A new appraisal of Sri Lankan BB zircon as a reference material for
661 LA-ICP-MS U-Pb geochronology and Lu-Hf isotope tracing: Geostandards and
662 Geoanalytical Research, v. 41, p. 335–358, doi:10.1111/ggr.12167.
663 Schmidt, J.M., Glen, J.M.G., and Morin, R.L., 2009, The Longview/Lakeview Barite Deposits,
664 Southern National Petroleum Reserve, Alaska (NPRA)—Potential-field Models and
665 Preliminary Size Estimates: USGS Professional Paper 1760–C, 29 p.

666 Shahab, B., Bashir, E., Kaleem, M., Naseem, S., and Rafique, T., 2016, Assessment of barite of
667 Lasbela, Balochistan, Pakistan, as drilling mud and environmental impact of associated
668 Pb, As, Hg, Cd and Sr: Environmental Earth Sciences, v. 75:1115, doi:10.1007/s12665-
669 016-5916-7.
670 Sircombe, K.N., and Stern, R.A., 2002, An investigation of artificial biasing in detrital zircon U-
671 Pb geochronology due to magnetic separation in sample preparation: Geochimica et
672 Cosmochimica Acta, v. 66, p. 2379–2397, doi:10.1016/S0016-7037(02)00839-6.
673 Stacey, J.S., and Kramers, J.D., 1975, Approximation of terrestrial lead isotope evolution by a
674 two-stage model: Earth and Planetary Science Letters, v. 26, p. 207–221,
675 doi:10.1016/0012-821X(75)90088-6.
676 Sundell, K.E., Gehrels, G.E., and Pecha, M.E., 2020, Rapid U-Pb geochronology by laser
677 ablation multi-collector ICP-MS: Geostandards and Geoanalytical Research,
678 doi:10.1111/ggr.12355.
679 Trenner, N.R., and Taylor, H.A., 1930, The solubility of barium sulphate in sulphuric acid: The
680 Journal of Physical Chemistry, v. 35, p. 1336–1344, doi:10.1021/j150323a015.
681 Woodhead, J., Hergt, J., Shelley, M., Eggins, S., and Kemp, R., 2004, Zircon Hf-isotope analysis
682 with an excimer laser, depth profiling, ablation of complex geometries, and concomitant
683 age estimation: Chemical Geology, v. 209, p. 121–135,
684 doi:10.1016/j.chemgeo.2004.04.026.

This is the peer-reviewed, final accepted version for American Mineralogist, published by the Mineralogical Society of America.
The published version is subject to change. Cite as Authors (Year) Title. American Mineralogist, in press.
DOI: https://doi.org/10.2138/am-2021-7436. http://www.minsocam.org/

FIGURE CAPTIONS

1. Doubly-terminated zircon crystals prior to milling in a ball mill. (A) Multiple grains in a polystyrene capsule in reflected light. (B) Three crystals on black paper in reflected light. (C) Backscattered electron image of a single crystal. (D) Backscattered electron image of the southwestern tip of the grain shown in panel C. Note the absence of microfractures on the surface of the crystal.
2. Reflected light photomicrographs of zircon after milling in a ball mill. (A) 10 minutes in air (UT1X). (B) 40 minutes in air (UT10X). White arrows point to broken tips. (C) 3 minutes in air then 3 minutes in isopropyl alcohol (UA1X). (D) Same procedure as for panel C, experiment UA10X. Milling in the titanium capsule imparted the metallic luster to the surfaces of the crystals in C and D. In all the experiments, milling broke through many tips and interiors.
3. Backscattered electron images of broken zircon grains after milling in a ball mill. (A and B) Experiment UT1X, 10 minutes total. (C and D) Experiment UT10X, 40 minutes total. (E and F) Experiment UA1X, 6 minutes total. (G and H) Experiment UA10X, 6 minutes total. Arrows point to microscopic fractures on the surfaces of the grains, which were not observed prior to milling (Fig. 1). Black splotches on grains in panels E-H are the remains of the carbon tape used to hold the grains during electron imaging.
4. Backscattered electron images of barite before and after boiling in a 0.94 M aqueous solution of sodium carbonate. (A) Fresh barite untreated with the sodium carbonate solution. (B) Barite grain after boiling for two hours. The white rectangle shows the location of panel C. (C) Close-up of the barite grain in panel B. The linear feature composed of barium carbonate suggests that fractures allow penetration of the solution into the interiors of grains. (D)

Barite grain after boiling for three hours. The barium carbonate crusts and the underlying mantle of partially-altered barite indicate that reaction 1 proceeded from the exteriors of the grains towards the interiors.

5. Backscattered electron images of barite grains after boiling in an aqueous solution of sodium carbonate for four or eight hours. This treatment completely converted the grains in each image to barium carbonate. The labels give the sodium carbonate concentrations and the boiling times. The scale is the same for all images.

6. Backscattered electron images of a large barite grain after participating in reactions 1 and 2. Reaction 1 took place during boiling in a 1.9 M aqueous solution of sodium carbonate for eight hours. Reaction 2 occurred during boiling in concentrated nitric acid for one hour. The white rectangle shows the location of panel B. The reactions left the grain scalloped at a scale of 10-20 μm and pitted at the micrometer scale.

7. Backscattered electron (A and B) and secondary electron (C and D) images of the surface of a large zircon crystal before and after boiling for eight hours in a 1.9 M sodium carbonate solution. Boiling removed contaminants from the surface and cracks but did not visibly affect the zircon crystal itself. The surface damage visible in the bottom half of the images is an identifying mark that we inscribed. The scale is the same for all images.

8. Backscattered electron (A and B) and secondary electron (C and D) images of the surface of a large zircon crystal before and after boiling for one hour in concentrated nitric acid. Boiling removed contaminants from the surface and cracks but did not visibly affect the zircon crystal itself. The surface damage visible in the bottom right of the images is an identifying mark that we inscribed. The scale is the same for all images.

9. Backscattered electron (A and B) and secondary electron (C, D, E, and F) images of the surface of a large zircon crystal before and after boiling in sodium carbonate solution for eight hours followed by boiling in concentrated nitric acid for one hour. The concentration of the sodium carbonate solution was 1.9 M. There is one scale for panels A, B, C, and D and a second scale for panels E and F.
10. Reflected light photomicrographs of grains separated from a natural sandstone sample (A) before and (B) after treatment with reactions 1 and 2. In panel A, there is so much barite that it is difficult to identify zircon. Panel B shows that the treatment removed barite, allowing many zircon crystals to be readily visible (arrows). The white mineral is quartz.

TABLES

1. Set-up and results of our ball mill experiments on mixtures of barite and zircon.
2. Summary of results of U-Pb and Lu-Hf isotope analyses of zircon.

SUPPLEMENTARY TABLES

S1. Standard reference zircon U-Pb and Lu-Hf information.

S2. Zircon U-Pb isotope data.

S3. Zircon Lu-Hf isotope data.

SUPPLEMENTARY FIGURES

S1. Comparison of $^{206}Pb/^{238}U$ dates of standard reference zircon not subjected to any chemical treatments (top row) to $^{206}Pb/^{238}U$ dates of standard reference zircon after boiling in concentrated nitric acid only (middle row) and sodium carbonate solution followed by concentrated nitric acid

753 (bottom row). The heights of the weighted mean (95% confidence) and published age (2-sigma)
754 bars indicate the uncertainties. The means were weighted by data point errors only.
755
756 S2. $^{206}Pb/^{238}U$ dates of boiled standard reference zircon without comparison to dates from
757 untreated zircon. The heights of the weighted mean (95% confidence) and published age (2-
758 sigma) bars indicate the uncertainties. The means were weighted by data point errors only. SL:
759 Sri Lanka.
760
761 S3. Comparison of our measured $^{176}Hf/^{177}Hf$ ratios of standard reference zircon not subjected to
762 any chemical treatments (top row) to $^{176}Hf/^{177}Hf$ ratios of standard reference zircon after boiling
763 in concentrated nitric acid only (middle row) and sodium carbonate solution followed by
764 concentrated nitric acid (bottom row). We did not experiment on 91500 or Temora; analyses of
765 the untreated grains are included in this figure for completeness. The heights of the weighted
766 mean (95% confidence) and published age (2-sigma) bars indicate the uncertainties. The means
767 were weighted by data point errors only. MT: Mud Tank. SL: Sri Lanka. Ples: Plesovice.

TABLE 1. SET-UP AND RESULTS OF MILLING EXPERIMENTS

Experiment number	Capsule composition	Capsule interior medium	Volume barite: Volume zircon	Total milling time (min)	Fraction of zircon grains lost during milling (%)	Fraction of remaining zircon grains that were broken (%)
In UTChron Laboratory						
UT1X	polystyrene	air	1:1	10	24	41
UT10X	polystyrene	air	10:1	40	49	57
In Arizona LaserChron Center						
UA1X	titanium	air, isopropanol	1:1	6	36	64
UA10X	titanium	air, isopropanol	10:1	6	30	23

TABLE 2. ZIRCON ISOTOPIC ANALYSES RESULTS SUMMARY

Zircon name	Weighted mean $^{206}Pb/^{238}U$ date (Ma)	95% confidence interval (Ma)	Number of analyses	MSWD	t-test p-value	Data sources for t-test	Weighted mean $^{176}Hf/^{177}Hf$	95% confidence interval	Number of analyses
Standards analyzed during our mass spectrometry session: no chemical treatment									
FC-1	1099	2	62	2.3	-	-	0.282171	0.000017	13
Mud Tank	-	-	-	-	-	-	0.282519	0.000023	8
Sri Lanka	-	-	-	-	-	-	0.281664	0.000031	8
R33	418	3	11	3.4	-	-	0.282739	0.000017	12
Plesovice	-	-	-	-	-	-	0.282484	0.000011	8
91500	-	-	-	-	-	-	0.282318	0.000035	8
Temora	-	-	-	-	-	-	0.282651	0.000012	8
Experiment: boiling in nitric acid only									
Nit-FC-1	1093	6	12	3.5	5.9E-02	1, 2	0.282157	0.000028	10
Nit-Mud Tank	not measured[a]	-	-	-	-	-	0.282518	0.000025	10
Nit-Sri Lanka	556	2	12	1.5	1.9E-06	2, 3, 4, 5	0.281655	0.000018	10
Nit-R33	416	2	11	2.6	1.0E-01	1, 2	0.282726	0.000018	12
Nit-Plesovice	338	1	12	0.93	9.4E-01	2	0.282474	0.000021	9
Experiment: boiling in sodium carbonate solution then nitric acid									
Sod-FC-1	1090	4	10	1.3	1.8E-03	1, 2	0.282143	0.000028	11
Sod-Mud Tank	not measured[a]	-	-	-	-	-	0.282508	0.000012	10
Sod-Sri Lanka	555	3	12	3.8	2.2E-04	2, 3, 4, 5	0.281641	0.000018	10
Sod-R33	414	2	11	2.2	4.3E-04	1, 2	0.282724	0.000021	10
Sod-Plesovice	336	1	12	1.5	2.6E-02	2	0.282485	0.000020	10

[a]The Mud Tank standard reference zircon was not used to test for disturbance to the U-Pb isotopic system.

1: This paper (Table S2). 2: Sundell et al. (2020). 3: Martin et al. (2015). 4: Cui et al. (2016). 5: Martin et al. (2020).

MSWD	t-test p-value
2.9	-
3.5	-
6.1	-
2.4	-
0.4	-
4.6	-
0.9	-
6.6	0.24
6.8	0.86
2.7	0.87
3.0	0.44
4.0	0.29
5.4	0.042
1.5	0.43
3.0	0.19
3.3	0.64
4.6	0.95

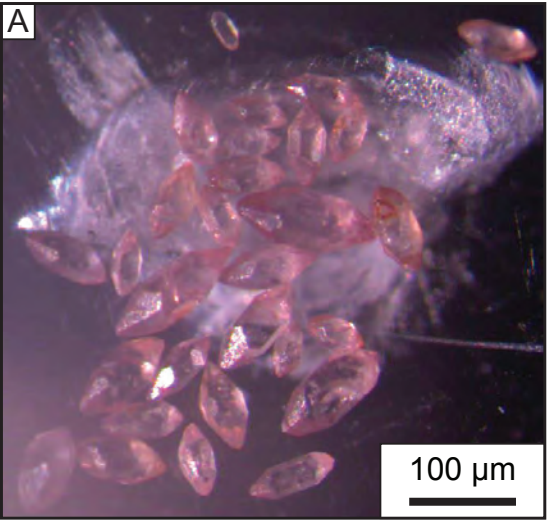

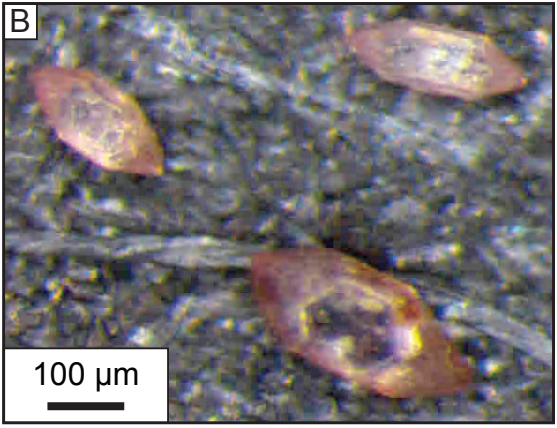

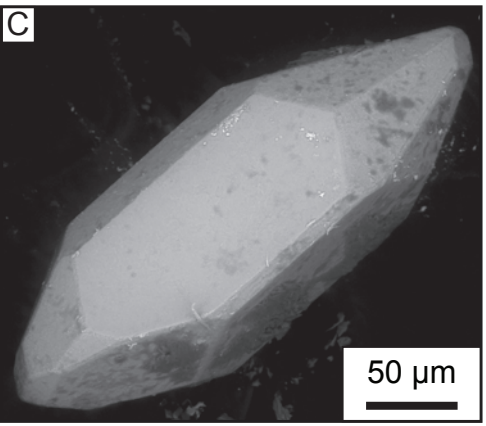

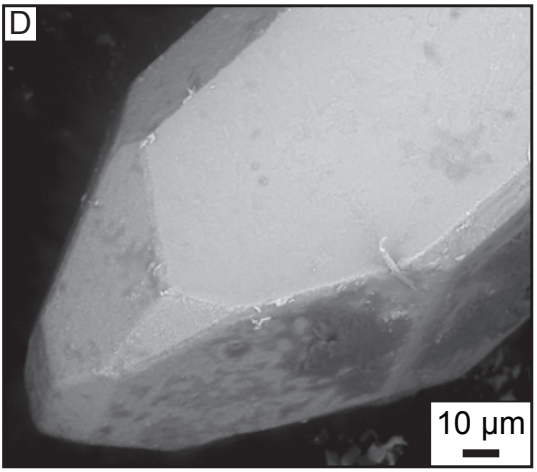

Figure 1 (Martin et al.)

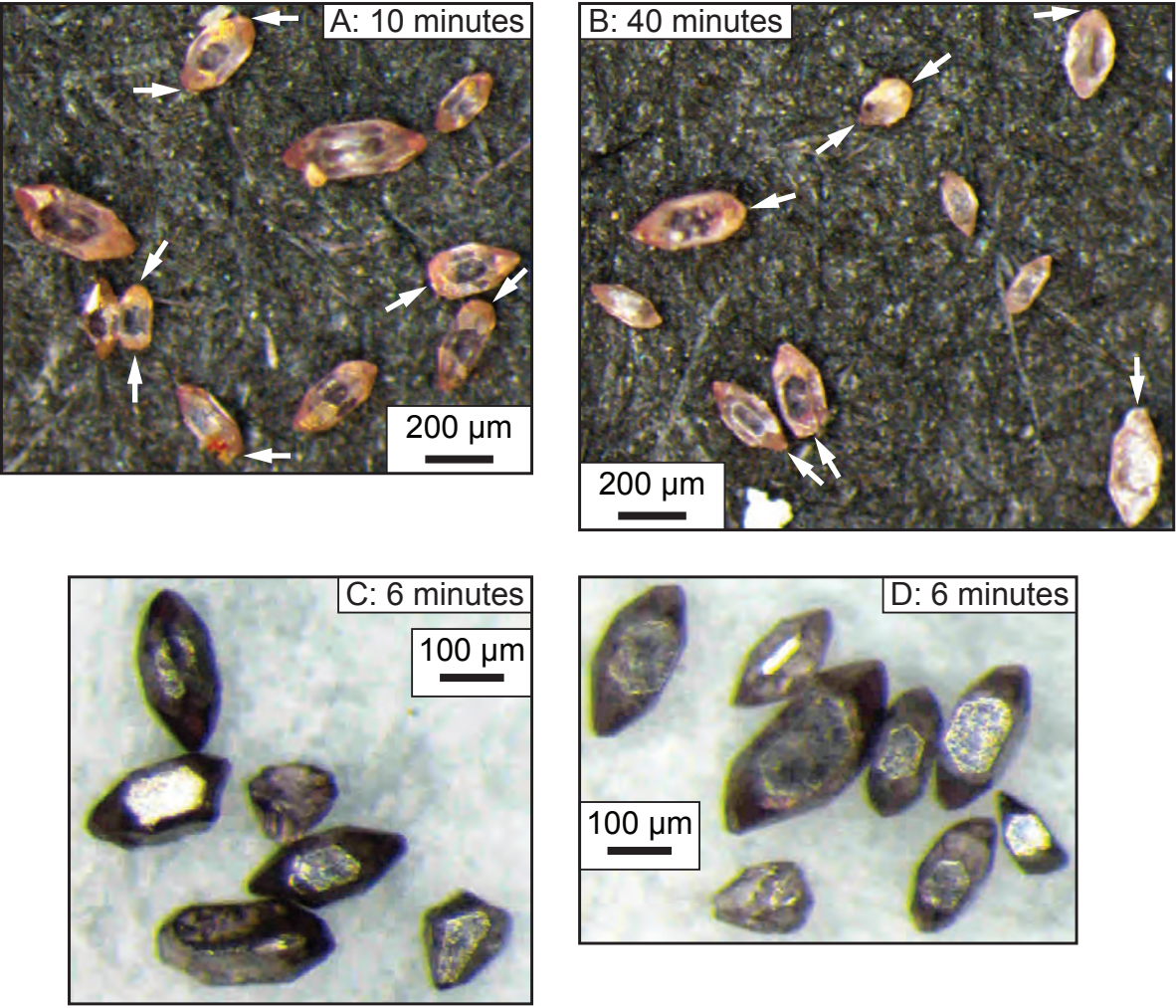

Figure 2 (Martin et al.)

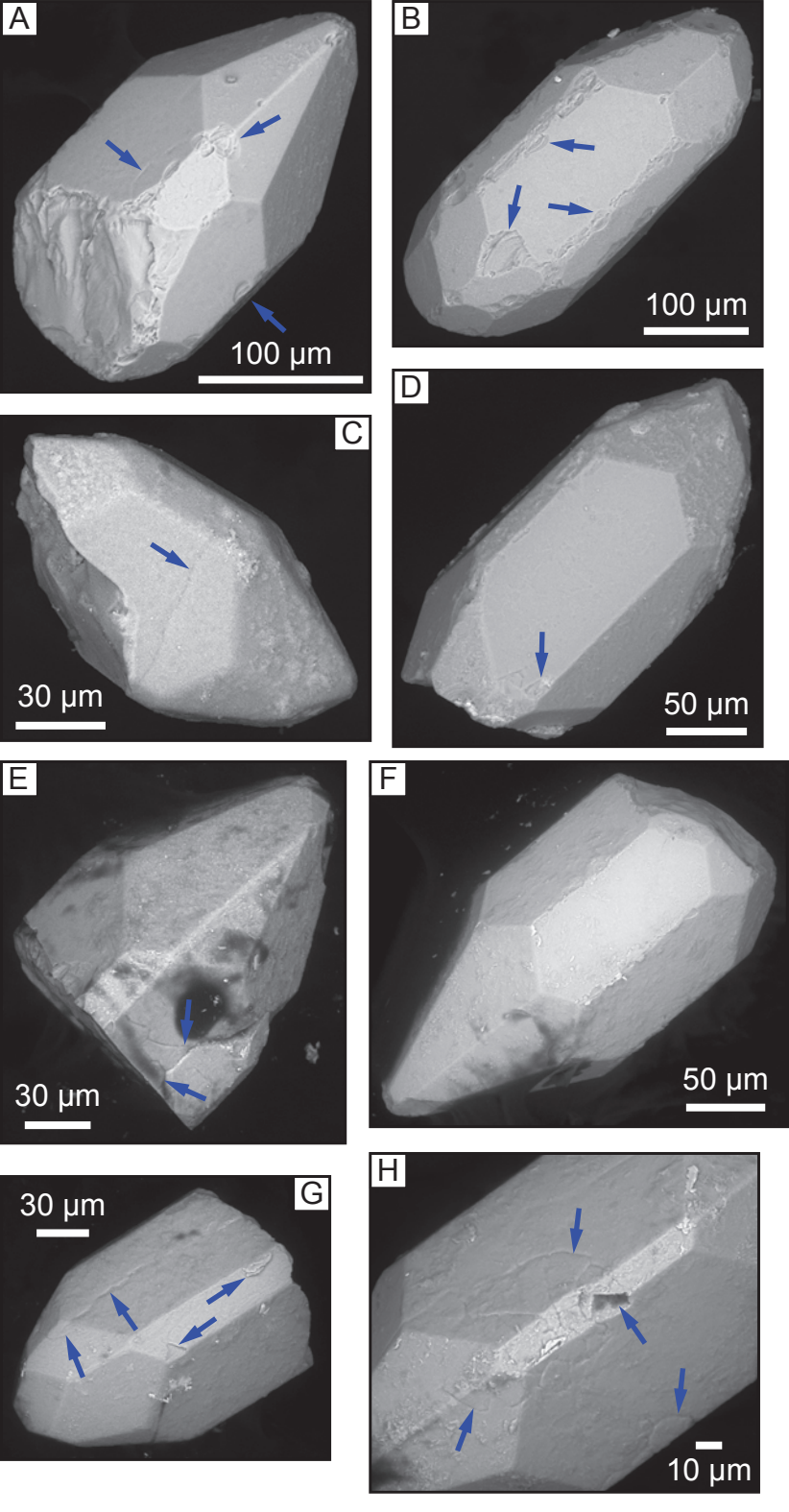

Figure 3 (Martin et al.)

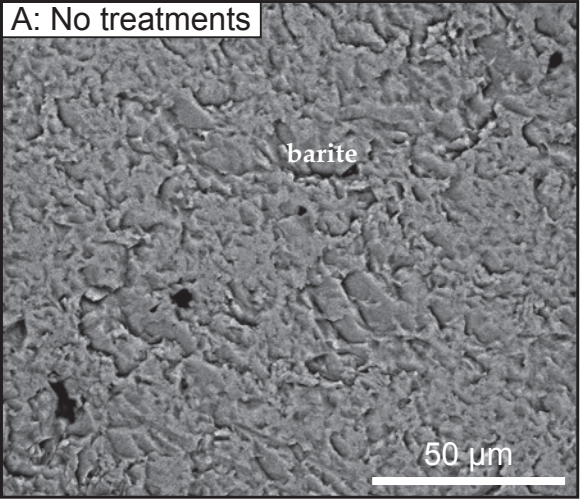

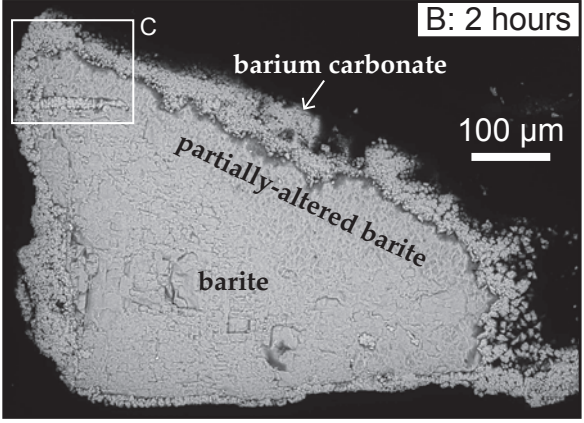

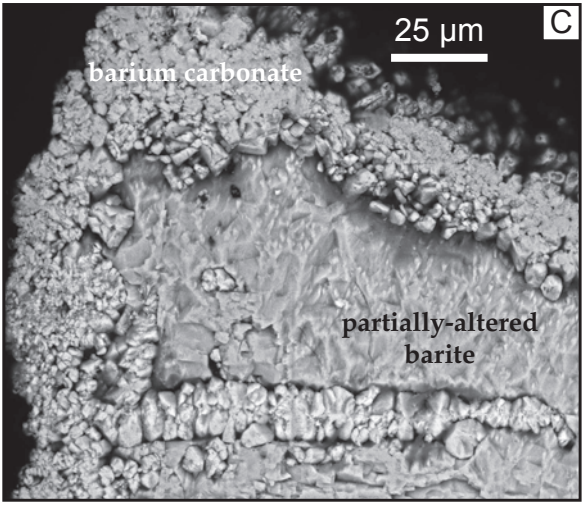

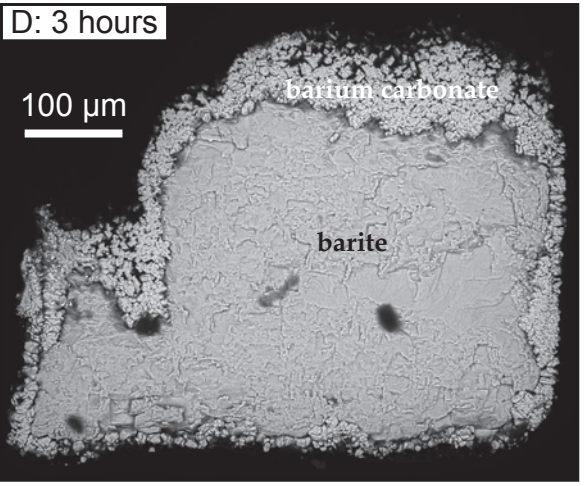

Figure 4 (Martin et al.)

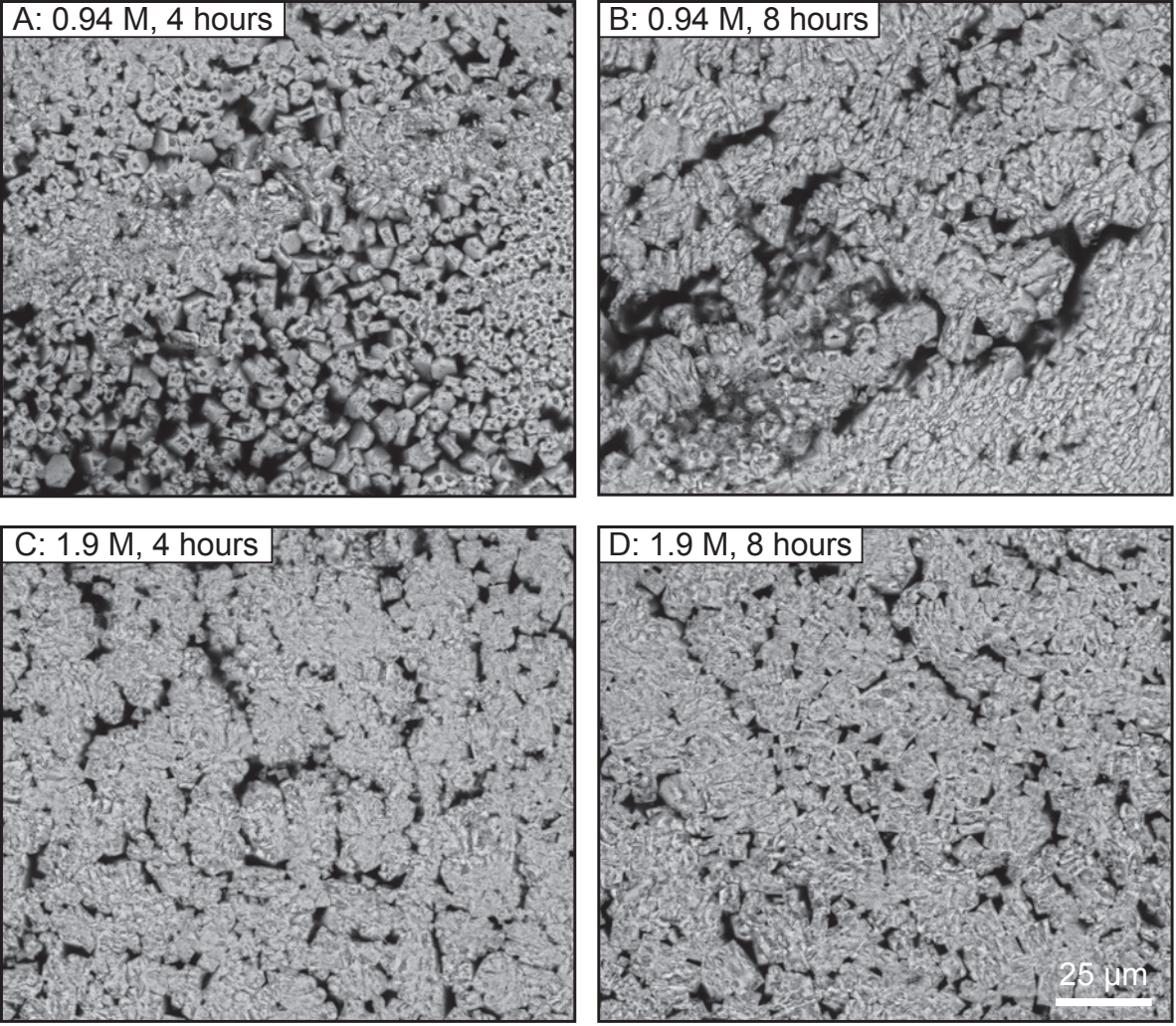

Figure 5 (Martin et al.)

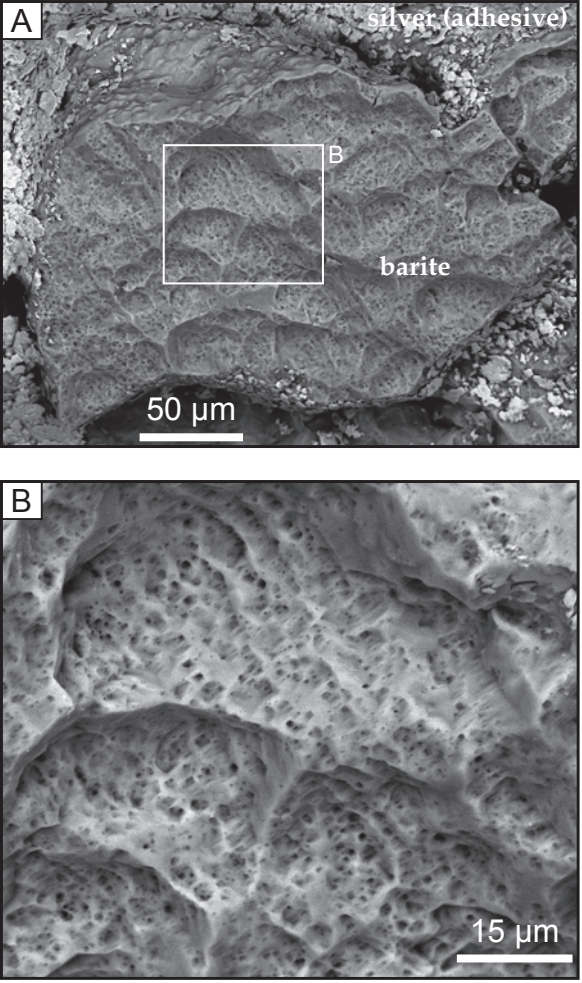

Figure 6 (Martin et al.)

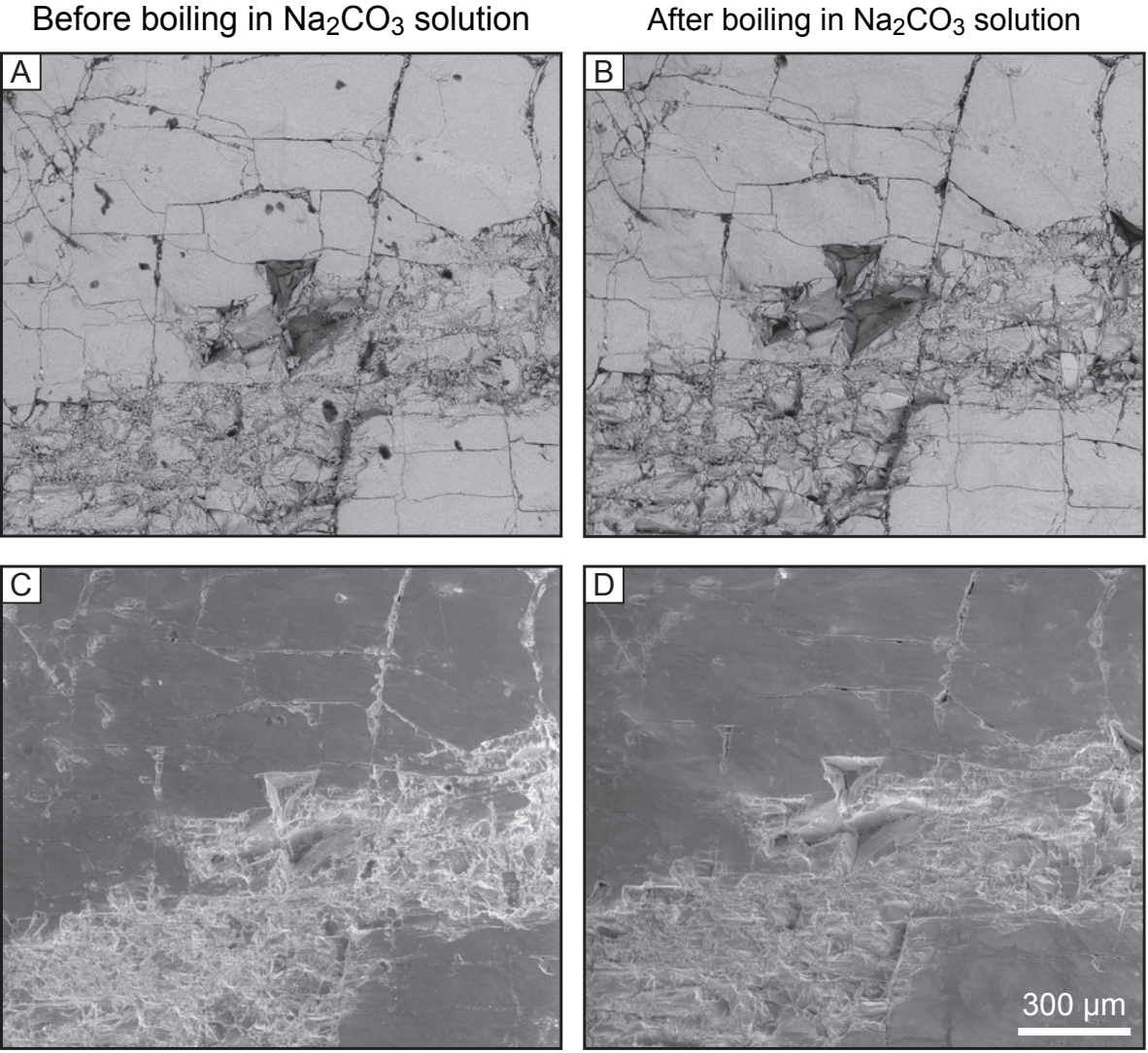

Figure 7 (Martin et al.)

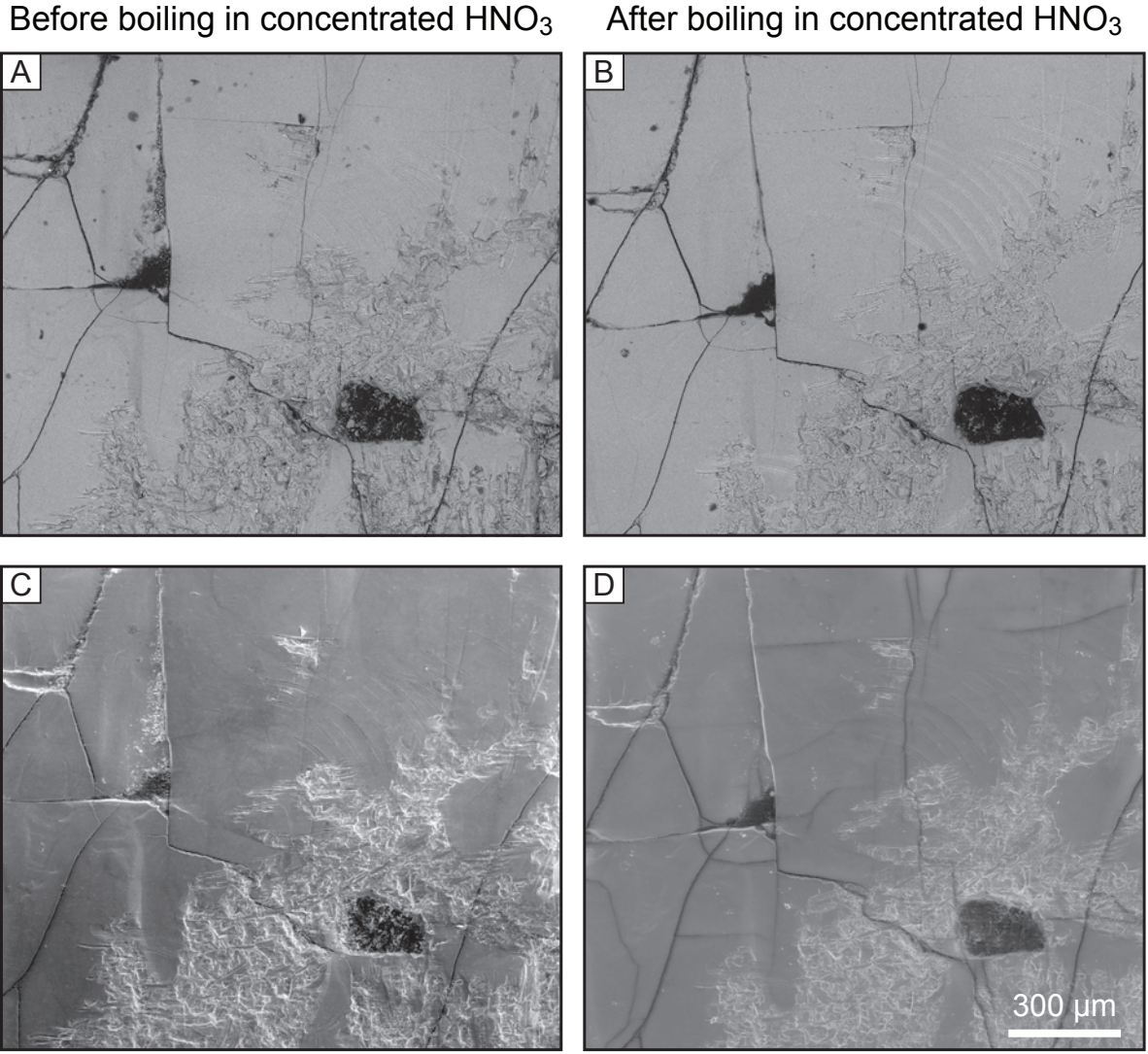

Figure 8 (Martin et al.)

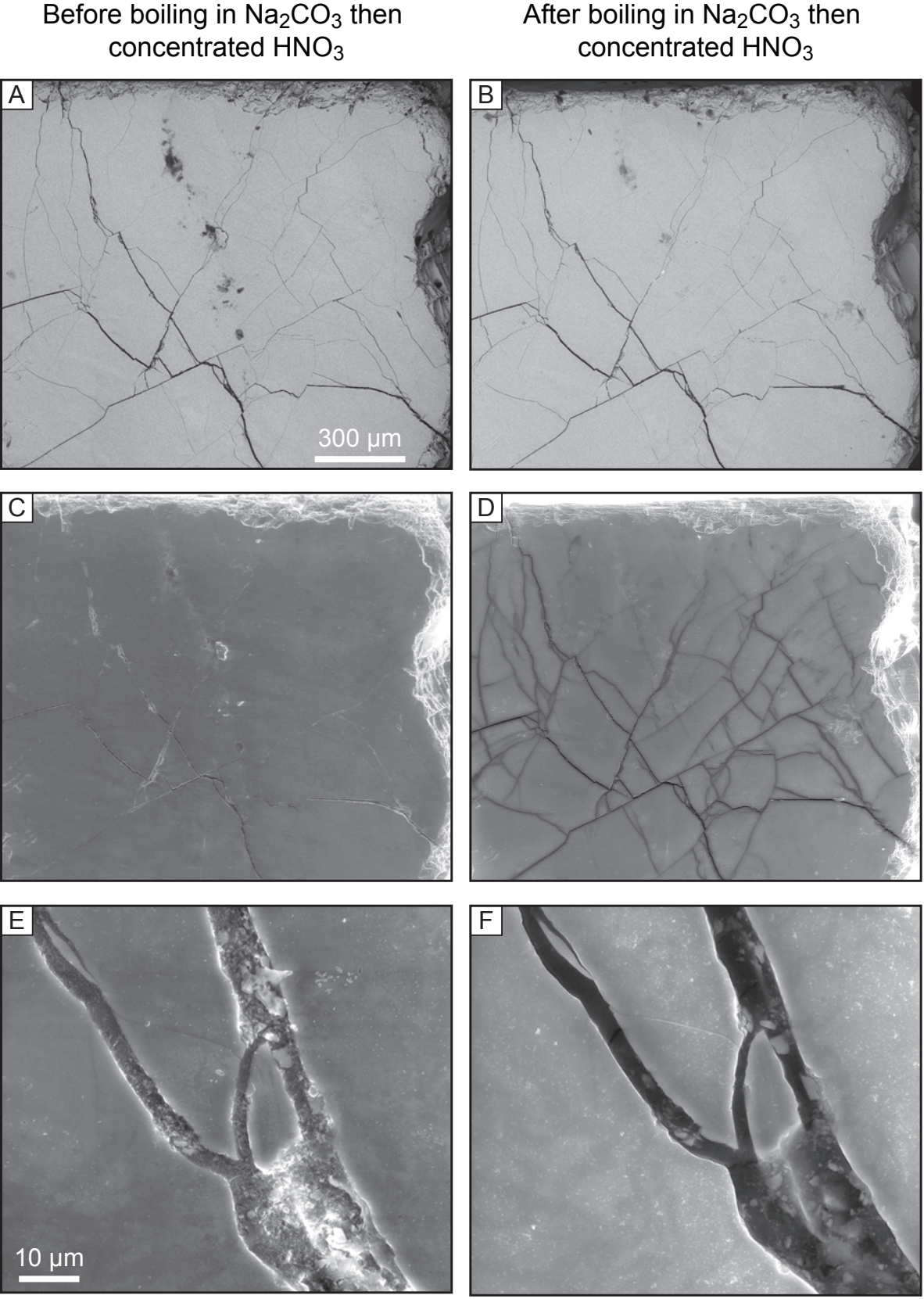

Figure 9 (Martin et al.)

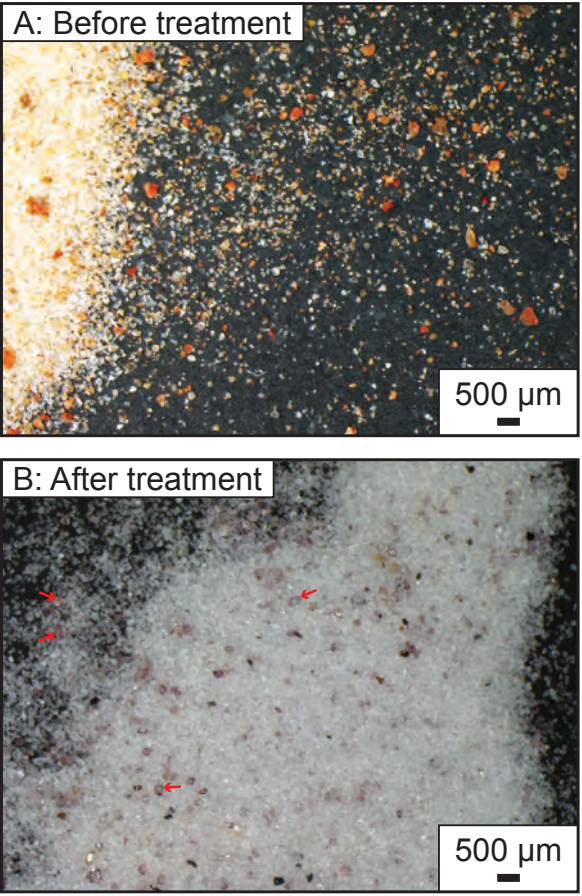

Figure 10 (Martin et al.)